ChemPubSoc Europe

DOI: 10.1002/open.201800284

Open Access ChemistryOPEN Full Papers

Special Collection

Ring-Stacking Water Clusters: Morphology and Stabilities

Liu Yang,[a] Hanyang Ji,[a] Xiaojie Liu,*[a, b] and Wen-Cai Lu[c]

The structures and interaction energies of water clusters with ring stacking motifs are studied by using ab initio calculations. The structures of the water clusters are constructed by stacking either single rings or multi-rings of tetramer, pentamer, and hexamer. We found that, in the single-ring-stacking motif, the most stable isomers exhibit an alternative clockwise-anticlockwise stacking pattern. We also show that four-layer single-ring-stacking isomers are not energetically favorable in comparison with those of two-layer multi-ring-stacking isomers. The relative stability of the isomers is also analyzed in terms of H-bond strength and elastic distortions of the water molecules.

Introduction

It is well known that the lowest-energy structures of a water tetramer[1–3] and pentamer[1–3] are cyclic structures in which each water molecule acts simultaneously as a single-proton-donor and a single-proton-acceptor to form two hydrogen bonds (H-bonds). The structure of the hexamer is more complex representing a transition from two-dimensional to three-dimensional geometries, and has been studied extensively by theoretical calculations[4–10,13–15] and experiments.[11,12] There are a large number of energetically competing isomers for the hexamer, including ring, book, bag, prism, cage, and boat structures. While experimental investigation by Liu et al.[11] showed that the lowest-energy water hexamer is a cage configuration. Recently, by using rotational spectroscopy experimental technique, Pérez et al.[12] found structures of cage, prism, and book isomers of water hexamer can be coexisted. Since the experiment was done in gas phase, the structures identified by their experiment are very reliable which is comparable to in-vacuo predictions. However, the monocyclic water hexamer is also important because it is the smallest possible ice-like clusters and its detailed study should provide important insights into the properties of bulk ice. Monocyclic isomer, although it exhibits higher energy, was also identified for water hexamer by Nauta et al.[13] These experiments allow us to explore some of the rich structural landscape that has been identified by theoretical calculations. Extensive *ab initio* calculations showed that the energy orders of various isomers of the hexamer are very sensitive to the levels of calculation methods and the treatment of various corrections such as zero point energy (ZPE) and basis set superposition error (BSSE) corrections.[4–10,14–16]

It has been shown that monocyclic water clusters can have chiral or achiral arrangements. Chiral arrangements exclusively feature water molecules that both donate and accept exactly one hydrogen bond within the ring-like network topology, whereas achiral cyclic deviate from this simple rule. Thus the intermolecular hydrogen bonding interactions of water are responsible for many remarkable physical properties of the liquid and solid phases of the compound and furthermore play a pivotal role in solution chemistry and biochemistry. For example, recently, Meng et al[17] reported the real-space observation of concerted proton tunneling in a cyclic water tetramer using a cryogenic scanning tunneling microscope. Low-temperature scanning tunneling microscopy also showed concerted tunneling of four protons within chiral cyclic water tetramers on an inert surface.[18] By using molecular orbital analysis, Wang et al[19–20] systematically examined hydrogen bond strength and concerted proton transfer process for bilayer 3,4,5-membered ring water clusters. Their theoretical studies provide new insights into the mechanism of chiral recognition in small water clusters, especially for monocyclic water clusters, at the atomic level. Recently, an accurate and efficient computational protocol, i.e., second order approximation of Møller–Plesset perturbation theory (MP2) and Coupled Cluster Singles and Doubles (Triple) (CCSD(T)) based on perturbative method, for characterization of waters clusters is reviewed by Tschumper et al.[21] and Xantheas et al.[22] Some of these high-level studies showed the electronic structure of water clusters as large as $(H_2O)_{17}$. Accurate energetics of hydrogen bonds in water clusters are important not only for the development of interaction potentials for water, but also for assessing the accuracy of other theoretical approaches.

It has also been proposed that the small cyclic water clusters (tetramer, pentamer and hexamer) are the basic

[a] L. Yang, H. Ji, Dr. X. Liu
Center for Quantum Sciences and School of Physics
Northeast Normal University
Changchun, 130117, China
E-mail: liuxj100@nenu.edu.cn
[b] Dr. X. Liu
Center for Advanced Optoelectronic Functional Materials Research and Key Laboratory of UV Light-Emitting Materials and Technology of Ministry of Educations, Northeast Normal University
Changchun, 130024, China
[c] Prof. W.-C. Lu
State Key Laboratory of Theoretical and Computational Chemistry
Institute of Theoretical Chemistry, Jilin University
Changchun, Jilin 130021, PR China

Supporting information for this article is available on the WWW under https://doi.org/10.1002/open.201800284

An invited contribution to a Special Collection dedicated to Computational Chemistry

building units for larger ($n \leq 20$) water clusters, particularly when the size of the clusters n is a multiple of 4, 5 or 6. For example, the lowest-energy isomers of water clusters $(H_2O)_{8,10,15}$ have been reported to be formed by stacking the tetramers or pentamers.[6–32] The structures of the water clusters $(H_2O)_{12,18,20}$ also follow the ring-stacking motif but the lowest-energy isomers are still a subject of debate due to the existence of various possible energetically competing ring-stacking isomers.[26–43] For $(H_2O)_{12}$, a fused cubic structure by stacking three tetramers is favored by most of the theoretical calculations,[27,29,32–35,38] but an isomer composed of two hexamers has also been proposed.[39,41] Using empirical potential models such as extended simple point charge (SPC/E) and atom-bond electro-negativity equalization method fused with molecular mechanics (ABEEM/MM), Kabrede et al.[41] and Yang et al.[39] proposed that the most stable isomer of water cluster $(H_2O)_{18}$ is a three 6-rings stacking structure. However, Hartke et al.[5] and Kabrede et al.[41] showed that the lowest-energy structure of $(H_2O)_{18}$ consists of a two-layer stacking of 4-5-4-multi-rings by employing four point transferable intermolecular (TIP4P) and flexible, polarizable, Thole-type interaction potential (TTM2-F) models, respectively. Furthermore, four major low-energy motifs for water clusters $(H_2O)_{20}$, i.e., edge-sharing pentagonal prism, face-sharing pentagonal prism, fused cubes, and dodecahedron have been studied extensively by ab initio calculations[27–32,35–39] and empirical potential calculations,[5,40–44] but no consensus has been reached on the ground-state structure of the water cluster.

As we can see from the above discussions that despite of extensive studies, the lowest-energy structures of these water clusters still remain elusive. Moreover, the optimum ring-stacking morphology is still not well understood. In this paper, we study the energetic stability of different isomers for water clusters $(H_2O)_{8,10,12,15,16,18,20,24}$ using quantum chemistry calculations at the level of Møller-Plesset perturbation theory. We show that although these clusters have many energetically competing isomers, the most stable isomers for these water clusters (except $(H_2O)_{16}$) are composed of either single-ring or multi-ring stacking with tetramer, pentamer, or hexamer as building units. We also found that the lowest-energy isomers of the single-ring stacking cluster all exhibit an alternative packing morphology in which the direction of H-bonding hydrogen atoms is clockwise-anticlockwise (c-a) for two-layer stacking, c-a-c for three-layer stacking and c-a-c-a for four-layer stacking. In addition, we show that for $(H_2O)_{16,20,24}$, four-layer single-ring stacking isomers are not energetically favorable as compared to the isomers with two-layer multi-ring stacking.

Results and Discussion

Due to the weak interaction nature of the water clusters, the accuracy of the calculations has to be considered carefully. It has been accepted that the second-order Møller-Plesset (MP2) using Valence triple-zeta basis set with diffuse and polarization functions is sufficient for water clusters based on the work by Klopper,[43–47] although for some subtle isomers higher levels of quantum chemistry calculations such as CCSD(T) may be required. While our present study used HF/6-311G(d,p) for structure optimization followed by single point energy calculation at the MP2/6-311++G(d,p) level, we have examined the reliability of methods and basis sets used in this paper by comparing the results of the water cluster $(H_2O)_{12}$ with those from higher level calculations. Specifically, we have also performed the geometry optimization for $(H_2O)_{12}$ using MP2/6-311++G(d,p) and then single point energy calculation at the MP4/6-311++G(d,p) level of theory. The results from the calculations at the different levels are compared in Table 1. The results show that the energy orders of the 5 isomers of $(H_2O)_{12}$ from the MP2/6-311++G(d,p)//HF/6-311G(d,p) and the MP4/6-311++G(d,p)//MP2/6-311++G(d,p) calculations are the same and the energy differences between the isomers are very similar. Therefore, the calculation method (i.e., MP2/6-311++G(d,p)//HF/6-311G(d,p)) used in this paper should be sufficient. The BSSE correction is not considered in our calculations because the basis set (6-311++G(d,p)) used in our calculations is large enough so that the BSSE is negligible according to the work of Kulkarni et al.[48] Note that zero-point energy correction is also not included here due to the heavy computational cost.

Table 1. Different levels of theory are compared for isomers of water cluster $(H_2O)_{12}$. Energies are given in eV.

Isomer	HF[a]	MP2[b]	MP2[c]	MP4[d]
$(H_2O)_{12-4a}$	0.000	0.000	0.000	0.000
$(H_2O)_{12-4b}$	0.013	0.011	0.011	0.011
$(H_2O)_{12-4c}$	0.026	0.022	0.022	0.023
$(H_2O)_{12-6a}$	0.113	0.051	0.044	0.071
$(H_2O)_{12-6b}$	0.125	0.065	0.056	0.084

[a] HF/6-311G(d,p). [b] MP2/6-311++G(d,p)//HF/6-311G(d,p). [c] MP2/6-311++G(d,p). [d] MP4/6-311++G(d,p)//MP2/6-311++G(d,p).

Basic Building Blocks

The monocyclic structures of water tetramer, pentamer and hexamer with each water monomer participating as a single hydrogen-bond donor and acceptor are displayed in Figure 1. Binding energies of these small water clusters obtained from our calculations at the MP2/6-311++G(d,p) level of theory are shown in Table 2. In these monocyclic structures the direction of the hydrogen atoms involved in the hydrogen bonding are arranged in a pattern that is clockwise (c) or anticlockwise (a)

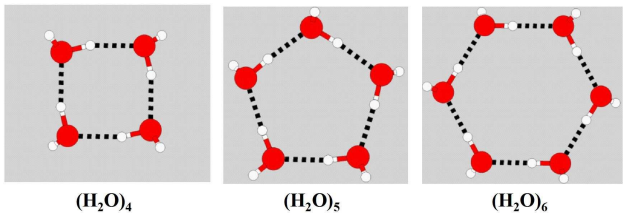

Figure 1. Monocyclic ring structures of water clusters $(H_2O)_{4,5,6}$ calculated at the MP2/6-311++G(d,p) level.

Table 2. Stacking sequences, binding energy per molecule (E_b/n in eV), relative binding energy with respect to the lowest-energy isomer (ΔE_b in eV), number of H-bonds within the layers ($(H–B)_{intra}$), number of H-bonds between the layers ($(H–B)_{inter}$), total number of H-bonds ($(H–B)_{total}$), ratio of the number of H-bonds within the layers *vs* the total number of H-bonds, and binding energy per H-bond (E_b/nH, in eV).

Isomer	Sequence	E_b/n	ΔE_b	Intra	Inter	Total	Ratio	E_b/nH
4	c	0.3395				4		0.3395
5	c	0.3606				5		0.3606
6	c	0.3739				6		0.3739
8a	c-a	0.4291	0.0000	8	4	12	66.67%	0.2860
8b	c-c	0.4289	0.0017	8	4	12	66.67%	0.2859
10a	c-a	0.4440	0.0000	10	5	15	66.67%	0.2960
10b	c-c	0.4435	0.0053	10	5	15	66.67%	0.2956
12–6a	c-a	0.4564	0.0000	12	6	18	66.67%	0.3043
12–6b	c-c	0.4553	0.0133	12	6	18	66.67%	0.3035
12–4a	c-a-c	0.4607	0.0000	12	8	20	60.00%	0.2764
12–4b	a-c-c	0.4598	0.0108	12	8	20	60.00%	0.2759
12-4c	c-c-c	0.4589	0.0217	12	8	20	60.00%	0.2753
15a	c-a-c	0.4765	0.0000	15	10	25	60.00%	0.2859
15b	a-c-c	0.4756	0.0122	15	10	25	60.00%	0.2854
15c	c-c-c	0.4744	0.0308	15	10	25	60.00%	0.2846
18a	c-a-c	0.4863	0.0000	18	12	30	60.00%	0.2918
18b	a-c-c	0.4852	0.0190	18	12	30	60.00%	0.2911
18c	c-c-c	0.4765	0.1756	18	12	30	60.00%	0.2859
16a	c-a-c-a	0.4773	0.0000	16	12	28	57.14%	0.2728
16b	c-c-a-c	0.4768	0.0085	16	12	28	57.14%	0.2725
16c	c-a-a-c	0.4762	0.0184	16	12	28	57.14%	0.2721
16d	c-c-a-a	0.4761	0.0203	16	12	28	57.14%	0.2720
16e	a-c-c-c	0.4756	0.0279	16	12	28	57.14%	0.2718
16f	c-c-c-c	0.4751	0.0364	16	12	28	57.14%	0.2715
16–m	c-a	0.4798	−0.0395	18	8	26	69.23%	0.2953
20a	c-a-c-a	0.4940	0.0000	20	15	35	57.14%	0.2823
20b	c-c-a-c	0.4930	0.0196	20	15	35	57.14%	0.2817
20c	a-c-c-c	0.4922	0.0374	20	15	35	57.14%	0.2812
20d	c-c-a-a	0.4921	0.0386	20	15	35	57.14%	0.2812
20e	c-c-c-c	0.4913	0.0548	20	15	35	57.14%	0.2807
20f	c-a-a-c	0.4908	0.0654	20	15	35	57.14%	0.2804
20–m	c-a	0.4959	−0.0378	24	10	34	70.59%	0.2917
24a	c-a-c-a	0.5025	0.0000	24	18	42	57.14%	0.2871
24b	c-c-a-c	0.5017	0.0196	24	18	42	57.14%	0.2867
24c	c-a-a-c	0.5015	0.0253	24	18	42	57.14%	0.2865
24d	c-c-a-a	0.5008	0.0399	24	18	42	57.14%	0.2862
24e	a-c-c-c	0.5007	0.0429	24	18	42	57.14%	0.2861
24f	c-c-c-c	0.5000	0.0609	24	18	42	57.14%	0.2857
24–m		0.5033	−0.0182	30	12	42	71.43%	0.2876

from outside to inside or from inside to outside view taking the paper as datum plane. In our present study of ring-stacking structures for large clusters, we will take the monocyclic structures of the water tetramer, pentamer, and hexamer as the building units. For a cluster of given size, we consider all possible stacking sequences of the monocyclic 4-, 5-, and 6-membered rings with different hydrogen bonding directions (clockwise (c) or anticlockwise (a)) in order to determine which stacking pattern is energetically favorable. We have also compared the relative energetic stabilities of the clusters composed of either single-ring or multi-ring stacking.

Two-layer stacking. There are three possible two-layer stacking structures for each of the $(H_2O)_{8,10,12}$ using the tetramer, pentamer, or hexamer respectively as the stacking units. Since the isomers with c-a and a-c stacking sequences are chiral isomers and degenerate in energy, there are only two different isomers for each two- layer stacking clusters as shown in Figure 2. We found that in the lowest-energy two-layer stacking isomers, the hydrogen atoms involved in the hydrogen bonding in the monocyclic 4-, 5-, and 6-ring are arranged in a clockwise-anticlockwise (c-a) pattern for the bottom-top layers respectively from the top view. The c-a two-layer stacking structures of $(H_2O)_8$ and $(H_2O)_{10}$ are also the lowest-energy isomers of these two clusters. For $(H_2O)_{12}$, although the c-a stacking is the lowest-energy structure among the motif of two hexamers stacking, it is not the lowest-energy structure for $(H_2O)_{12}$ as we will discuss later in this paper. We can see that for two-layer single-ring stacking structures, the most stable isomers at the MP2/6-311++G(d,p) level are those with the c-a stacking pattern, followed by c-c (or a-a) stacking.

Three-layer stacking. There are three non-equivalent ways (c-a-c, a-c-c, and c-c-c) for three 4-, 5-, or 6-membered rings to stack in three-layers to form the $(H_2O)_{12,15,18}$ clusters. The most stable isomers of the $(H_2O)_{12,15,18}$ clusters in the three-layer stacking structures are all with the direction of H-bonding hydrogen atoms being clockwise-anticlockwise-clockwise (c-a-c) from the top view, as plotted in Figure 3. The c-a-c structures are not only the lowest-energy structures in the ring-stacking motif, but also the lowest-energy structures for these clusters. Our MP2/6-311++G(d,p) calculations also show that the structures with a-c-c stacking are energetically more favorable than the c-c-c stacking for $(H_2O)_{12,15,18}$, as one can see from

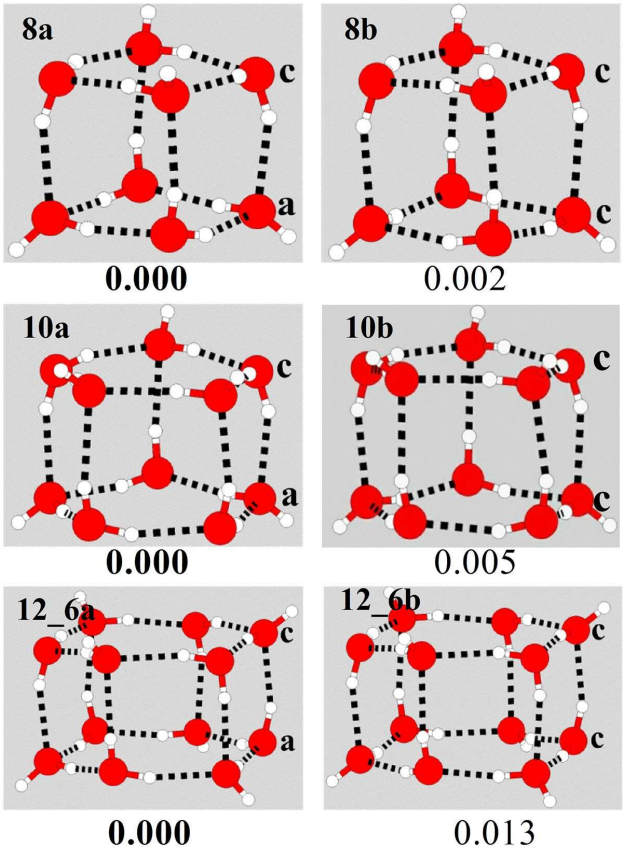

Figure 2. All possible isomers of water cluster $(H_2O)_{8,10,12}$ in the two-layer single-ring stacking motif, along with relative binding energy (ΔE_b) with respect to the corresponding lowest-energy isomers obtained at the MP2/6-311++G(d,p) level. Stacking sequences are labeled on the right of the structures, respectively ("c" indicates clockwise and "a" stands for anticlockwise).

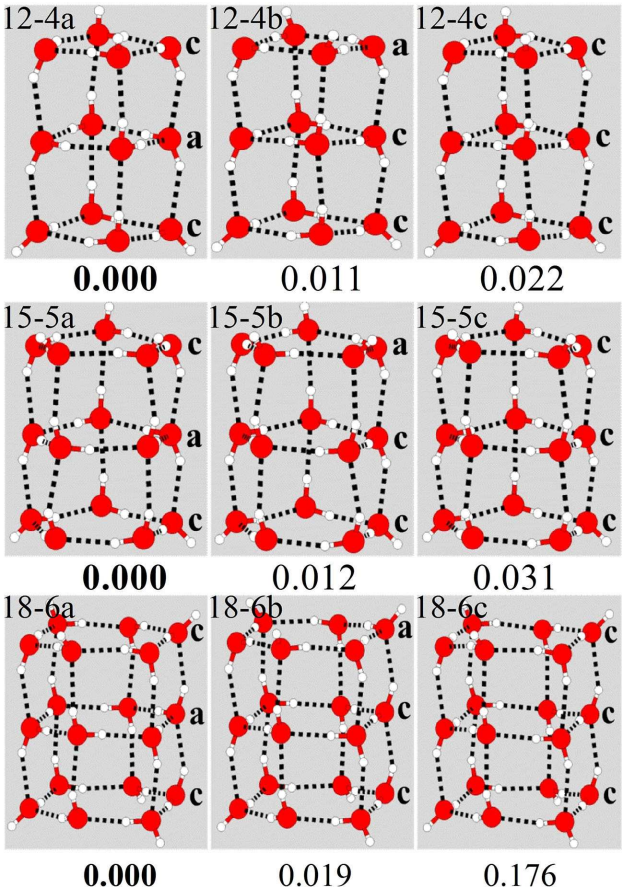

Figure 3. All possible isomers of water clusters $(H_2O)_{12,15,18}$ in the 3-layer single-ring stacking motif, along with relative binding energy (ΔE_b) with respect to the corresponding lowest-energy isomers obtained at the MP2/6-311++G(d,p) level. Stacking sequences are labeled on the right of the structures, respectively ("c" indicates clockwise and "a" stands for anticlockwise).

Figure 3 where the relative energies of the three different stacking sequences for these clusters are also given. The binding energies of these three-layer stacking structures are also listed in Table 2.

Four-layer stacking. There are six non-equivalent four-layer single-ring stacking structures for $(H_2O)_{16,20,24}$ using 4-, 5- and 6-membered rings, respectively. For $(H_2O)_{16}$, the lowest-energy isomer is the one with stacking sequence of c-a-c-a (Figure 4 (a)) followed by those with the stacking sequences of c-c-a-c, c-a-a-c, c-c-a-a, a-c-c-c, and c-c-c-c, respectively, from our calculations at the MP2/6-311++G(d,p) level. For $(H_2O)_{20}$, the energy of the isomer with c-a-c-a stacking pattern is also lower than that of other isomers with the stacking sequences of c-c-a-c, a-c-c-c, c-c-a-a, c-c-c-c, and c-a-a-c, by 0.010, 0.020, 0.021, 0.029, and 0.038 eV, respectively. It is interesting to note that the lowest-energy stacking (c-a-c-a pattern) observed for $(H_2O)_{16,20}$ is also the energetically favorable stacking for water cluster $(H_2O)_{24}$ composed of four 6-rings as one can see from Figure 4 and Table 2.

Multi-ring stacking. It should be noted that although the c-a-c-a four-layer stacking structures are the lowest-energy structures for $(H_2O)_{16,20,24}$ within the monocyclic stacking motif, they are not the lowest-energy structures for these clusters. As we will discuss below, the vertical hydrogen bonds between the stacking layers are generally weaker than those within the layers. Therefore, when the single-ring stacking structures have more than three stacking layers, the fraction of the weak H-bonds between the layers is too large and stability of the stacked structure is reduced. We found that for the $(H_2O)_{16,20,24}$ clusters, a two-layer multi-ring stacking motif becomes energetically more favorable as compared to the single-ring stacking motif. We have studied several stacking patterns for two-layer multi-ring stacking structures of $(H_2O)_{16,20,24}$. The isomers shown in Figure 5 are the lowest-energy ones we found within this stacking motif. It is interesting to note that the lowest-energy two-layer multi-ring stacking isomers of water clusters $(H_2O)_{16}$ and $(H_2O)_{20}$ also follow the alternating clockwise-anticlockwise stacking sequence for the outmost rings of the cluster. However, the lowest-energy multi-ring stacking isomers of $(H_2O)_{24}$ do not follow this alternating stacking pattern. We also note that the three-layer tetramer stacking structure of $(H_2O)_{12}$ shown in Figure 3 would also be viewed as a two-layer, 4-4 multi-ring stacking structure.

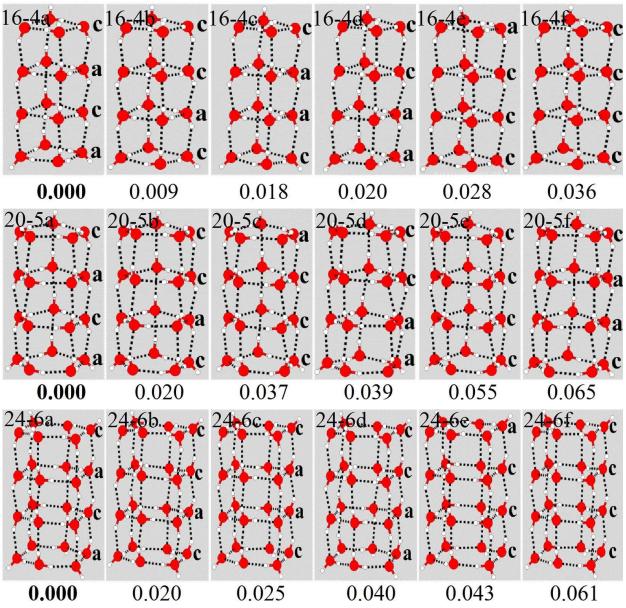

Figure 4. All possible isomers of water cluster $(H_2O)_{16,20,24}$ in the 4-layer single-ring stacking motif, along with relative binding energy (ΔE_b) with respect to the corresponding lowest-energy isomers obtained at the MP2/6-311++G(d,p) level. Stacking sequences are labeled on the right of the structures, respectively ("c" indicates clockwise and "a" stands for anticlockwise).

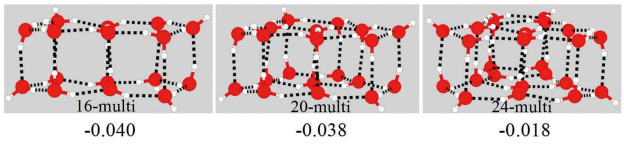

Figure 5. Low-energy isomers of water clusters $(H_2O)_{16,20,24}$ with multi-ring stacking motif, along with relative binding energy (ΔE_b) with respect to corresponding lowest-energy single-ring stacking isomers obtained at the MP2/6-311++G(d,p) level.

We try some 2-layer (2 L) multi-ring structural isomers for $(H_2O)_{18,20,24}$ as shown in Figure S1. The binding energies and relative energies with respect to the lowest-energy isomers are also shown below each structure. For water cluster $(H_2O)_{18}$, the relative energy of 2 L multi-ring (i.e., 2 L-4,5,4-ring (18b), 2 L-5,5,4-ring (18d)) is relatively higher than the lowest-energy isomer (18a) with 3 L single ring stacking motif by 0.0230 and 0.1057 eV, respectively. For water cluster $(H_2O)_{20,24}$, the structural isomers with 2 L multi-ring stacking (i.e., 2 L-5,5,5-ring (20a) and 2 L-5,5,5,4-ring (24a)) are energetic favorable and the total energies are lower than that of isomers with multi-layer single ring stacking by 0.0375 (i.e., 4 L-5-ring (20b)) and 0.0182 eV (4 L-6-ring (24b)), respectively, indicating that structural isomers with 2 L multi-ring stacking are energetically favorable. We note that although 2 L-5,5-ring isomer (16b) exhibits higher binding energy, it is the lowest-energy one within ring stacking motif. We only focus on lowest-energy structures of water clusters with ring staking motifs in this study. On the other hand, according to our structural analysis, distortion of the bond length and bond angle of the water molecules in 4-ring motif is very large and will cost elastic energy, leading to less stability. So structural isomer with 2 L multi-ring consisted of four tetramers will be not energetic favorable.

According to our previous study,[32] water clusters with larger than 3-layer single ring stacking are not energetic favorable. From Figure S1, we can also see that the relative energies for $(H_2O)_{16,20,24}$ isomer with 4 L-4,5,6-ring stacking motif are higher than the lowest-energy 2 L stacking structure by 0.0783, 0.0375 and 0.0122 eV, respectively, indicating again isomers with 4-layer single n-ring stacking are not stable. However, as will be discussed in the following subsection, $(H_2O)_{12,16}$ is better classified as 3 L-4-ring or 4 L-4-ring stacking because in this way the intra-layer hydrogen bonds are stronger than the inter-layer ones, consistent with the definition of the intra-layer and inter-layer hydrogen bonds in other water clusters studied in this paper. On the other hand, intra-layer and inter-layer hydrogen bonds defined like this is reasonable since concerted proton transfer process of intra-layer hydrogen bonds can be observed by vibrational circular dichroism spectrum from Wang's studies,[20] indicating that intra-layer hydrogen bonds are stronger. They also reported that the energy difference between isomer with clockwise-anticlockwise and clockwise-clockwise pattern are smaller. Our results is similar to the Wang's finding[20] that the energy difference between c-a and c-c patterns for $(H_2O)_{10,12,16}$ is less than 0.013 eV as discussed above.

General Trends of Relative Stability

From the energetic comparison as discussed above we see that the most stable isomers of the water clusters $(H_2O)_n$ in the range n = 8–24 within the single-ring stacking motif are those with alternating c and a ring-stacking sequences (i.e., c-a, c-a-c, and c-a-c-a for 2, 3, and 4 layers stacking, respectively). Moreover, we also found that when the stacking layers are less than four, the single-ring stacking structures are the lowest-energy structures of the corresponding clusters (i.e., $(H_2O)_{8,10,12,15,18}$). However, although the 4-layer alternative a-c-a-c stacking structures of $(H_2O)_{16,20,24}$ are the lowest-energy isomers of these clusters under the single-ring stacking motif, they are not energetically as competitive as those of the two-layer multi-ring stacking isomers. Nevertheless, these four-layer stacking structures are useful for understanding the stability of the water clusters with different H-bonding stacking pattern as we will discuss later in this subsection. In particular, we will show why the four-layer single-ring stacking structures are not as good as other structures for the water clusters.

The relative energetic stability of the ring-stacking isomers can be qualitatively understood by the competition between the energy gain due to the formation of the hydrogen bonds and stain energy loss due to the deformation of the water molecules upon the formation of the clusters.

The average lengths for the hydrogen bonds within the layers ($R_{intra}(O\cdots H)_{ave}$) and between the layers ($R_{inter}(O\cdots H)_{ave}$) for each ring-stacking isomer studied in this paper are plotted in Figure 6(a). The corresponding average bond angles for the

hydrogen bonds within the layers ($\angle_{intra}(O–H\cdots O)_{ave}$) and between the layers ($\angle_{inter}(O–H\cdots O)_{ave}$) are also plotted in Figure 6(b). We found that for all the single-ring stacking isomers except the higher-energy c-c stacking isomer of $(H_2O)_8$, the average bond lengths of the hydrogen bonds within the layers are shorter than those between the layers. Comparing to $\angle_{inter}(O–H\cdots O)_{ave}$, the average bond angles for the hydrogen bonds within the layers ($\angle_{intra}(O–H\cdots O)_{ave}$) are in also closer to that of the hydrogen bonds between a water dimer (178.2 degree). These results indicate that the hydrogen bonding is stronger within the layers but weaker between the layers. For the multi-ring stacking isomers of $(H_2O)_{16,20,24}$, the average bond lengths of the hydrogen bond within the layers are also shorter than those between the layers, similar to the cases of single-ring stacking isomers. However, there is no clear difference between the average bond angles for the hydrogen bonds within and between the layers in the multi-ring stacking isomers. The average value of the hydrogen bond angles in the multi-ring stacking isomers lies between the values $\angle_{intra}(O–H\cdots O)_{ave}$ and $\angle_{inter}(O–H\cdots O)_{ave}$ of the single-ring stacking isomers. We define the binding energy E_b of a $(H_2O)_n$ cluster as the energy difference between the total energy of the cluster and the energy of the n isolated water molecules. In Figure 6(c) and (d), we plot the binding energy per hydrogen bond E_b/nH as a function of the average H-bond length $R(O\cdots H)_{ave}$ and the deviation of the averaged bond angle $\Delta\theta$ with respect to that of the water dimer ($\Delta\theta = 178.2\text{-}\angle(O–H\cdots O)_{ave}$), respectively. We found that the E_b/nH decreases linearly with $R(O\cdots H)_{ave}$ and $\Delta\theta$. Least square fitting to the E_b/nH from all clusters and all isomers in this study as the function of $R(O\cdots H)_{ave}$ and $\Delta\theta$ yield $E_b/nH = 1.370 - 0.548 \times R(O\cdots H)_{ave}$, and $E_b/nH = 0.343 - 0.004 \times \Delta\theta$, respectively. The degree of the linear dependence of the E_b/nH on the $R(O\cdots H)_{ave}$ and $\Delta\theta$ can also be quantified using the Pearson Product-moment Correlation Coefficient (PMCC):

$$r_{xy} = \frac{1}{n}\sum_{i}^{n}(x_i - \bar{x})(y_i - \bar{y})/s_x s_y$$

where x and y represent $R(O\cdots H)_{ave}$ (or $\Delta\theta$ and E_b/nH, respectively, and S_x and S_y are their standard deviations. Our analysis shows that the PMCC for E_b/nH versus $R(O\cdots H)_{ave}$ and $\Delta\theta$ are −0.978 and −0.947 respectively, indicating they are strongly anti-correlated, i.e., E_b/nH increased as $R(O\cdots H)_{ave}$ and $\Delta\theta$ getting smaller.

We also note that the water molecules are distorted from its isolated structure when forming the water clusters. In an isolated water molecule, the bond length between the O and H is 0.941 Å and the bond angle of H–O–H is 105.4 degree from our calculation at the HF/6-311G(d,p) level. When the water molecules form the clusters, we classify the O and H atoms in each water molecule according to their different bonding environments. If one or both H atoms in the water molecule are involved in the H-bonding, we denote the O atom in this molecule as O_s or O_d respectively. Similarly, H_b and H_f indicate that the H atom is involved or not involved in the H-bonding. According to this classification, there should be three different types of possible chemical O–H bond length, (i.e., r_{sf}, r_{sb}, and r_{db}) and two types of bond angles (i.e., $\angle H_f–O_s–H_b$ and $\angle H_b–O_d–H_b$) in a water molecule, respectively. The average values of the three types of bond lengths and the two types of bond angles from most stable single-ring stacking and multi-ring stacking isomers studied in this paper are plotted in Figure 7(a) and (b), respectively. The results show that while the O–H bond length between the O and the non-H-bonding H (r_{sf}) is almost the same as that in the free water molecule, the O–H bond lengths increase when H atoms in water molecule are participating in H-bonding. In particular, when only one H atom in the water molecule is involved in the H-bonding, the average r_{sb} is about 0.957 Å which is about 1.7% longer than that of the isolated water molecule. The bond angles of the water molecules in the clusters are also larger than those of the isolated molecule. The molecules with only one H atom participating in the H-bonding (with $\angle H_f–O_s–H_b$) also exhibit larger bond angle distortion (about 1.2%) from that in the free molecule. This distortion will cost elastic energy although the formation of cluster will gain hydrogen bonding energies. In Figure 7(c) and (d), we plot the bonding energy per molecule (E_b/n) as the function of percentage of the root-mean-square deviation of the bond lengths and bond angles from that of a free water molecule, respectively. We find that the data points of E_b/n versus the relative O–H bond length distortions separate into two sets, with the data from the stacking isomers with 4-membered ring fall into one set and those from isomers with 5- and 6-membered rings go into another set. We find that E_b/n decreases almost linearly with distortions of bond length and bond angle with the PMCC values of −0.973 for E_b/n vs the relative O–H bond length distortions in the 4-membered rings-

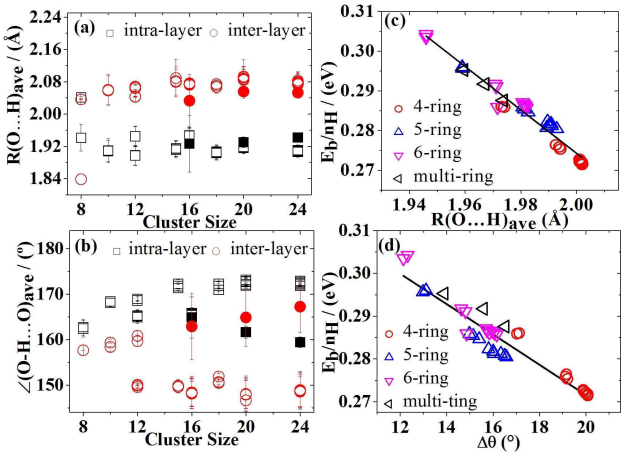

Figure 6. a) Average bond length of H-bonds within the layers and between the layers vs. water cluster size. b) Average bond angle of H-bonds within the layers and between the layers vs. water cluster size. c) Binding energy per H-bond (E_b/n_H) vs. average bond length of H-bonds ($R(O\cdots H)_{ave}$). d) Binding energy per H-bond (E_b/n_H) vs. the deviation of the averaged bond angle with respect to that of the water dimer $\Delta\theta = (178.2\text{-}\angle(O–H\cdots O)_{ave})$. a, b) Hollow squares and circles indicate intra-layer and inter-layer H-bonds in single ring stacking motif, respectively. Solid squares and circles indicate intra-layer and inter-layer H-bonds in multi-ring stacking motif, respectively. c, d) Hollow circles, up-triangles, down-triangles and left-triangles represents single 4, 5, 6-ring, and multi-ring stacking water clusters, respectively. Black lines represent fitted lines according to the calculations.

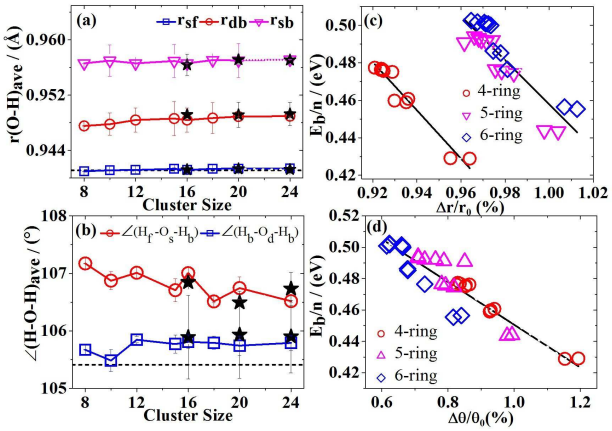

Figure 7. a) Average values of r(O–H) vs. water cluster size. b) Average values of ∠(H–O–H) vs water cluster size. c) Binding energy per molecule (E_b/n) vs. bond length relative distortion of r(O–H) ($\Delta r/r_0$), and Δr is calculated by $\Delta r = \sum_{i-l}^{M} \sqrt{\frac{(r_i - r_0)^2}{M}}$. d) Binding energy per molecule (E_b/n) vs. bond angle relative distortion of ∠(H–O–H) ($\Delta\theta/\theta_0$), and $\Delta\theta$ is calculated by $\Delta\theta = \sum_{i-l}^{M} \sqrt{\frac{(\theta_i - \theta_0)^2}{M}}$. Dash lines in (a) and (b) are bond length of O–H and bond angle of H–O–H in free water molecule, respectively. Black stars represent bond length and bond angle in multi-ring stacking isomers for $(H_2O)_{16,240,24}$, respectively. For detailed definitions, please refer to the text.

stacking isomers, −0.901 for E_b/n vs the relative O–H bond length distortions in the 5- and 6-membered-ring stacking isomers, and −0.924 for E_b/n vs the relative angle distortions. These results suggest that the distortion of the bond length and bond angle of the water molecules due to the formation of the clusters will cost elastic energy.

Within the single-ring stacking motif, different isomers of the clusters with same number of layers but different stacking sequences have the same number of hydrogen bonds within the layers and between the layers. However, we found the average H-bond lengths are generally smaller in the lowest-energy alternating stacking isomers as one can see from Table 3. Larger bond angles of the H-bond $\angle(O–H\cdots O)_{ave}$ are also energetically favorable. The deviation of the O–H bond length in the water molecule is generally smaller for the alternating stacking isomers too, but the deviation of the water molecule bond angles are not always the smallest for the lowest-energy single-ring stacking isomers when the number of water molecules in the cluster is less or equal to 12. These results indicate the strong contribution to the energetic stability of the clusters comes from the strength of the hydrogen bonds in the clusters. Distortion of the O–H bond length will cost more

Table 3. Average bond length and bond angle of H-bonds ($R(O\cdots H)_{ave}$ (Å) and $\angle(O–H\cdots O)_{ave}$ (°)), bond length and bond angle relative distortion of water molecule ($\Delta r/r_0$ and $\Delta\theta/\theta_0$), and the binding energies E_b (in eV) of the isomers.

Isomer	R(O···H)ave	∠(O–H···O)ave	$\Delta r/r_0$[a]	$\Delta\theta/\theta_0$[a]	E_b
8a	1.9731	161.0588	0.9553	1.1942	3.4325
8b	1.9740	161.1578	0.9640	1.1531	3.4309
10a	1.9590	165.0651	0.9978	0.9933	4.4399
10b	1.9591	165.2034	1.0040	0.9785	4.4346
12–6a	1.9459	165.8622	1.0069	0.8402	5.4770
12–6b	1.9460	166.0427	1.0126	0.8163	5.4637
12–4a	1.9926	159.0266	0.9404	0.9361	5.5284
12–4b	1.9938	159.0662	0.9290	0.9299	5.5176
12–4c	1.9942	158.9820	0.9262	0.9352	5.5068
15a	1.9807	163.2031	0.7809	0.9756	7.1469
15b	1.9813	163.0386	0.7925	0.9784	7.1347
15c	1.9826	162.7794	0.8182	0.9839	7.1161
18a	1.9707	163.5502	0.6777	0.9746	8.7529
18b	1.9712	163.3663	0.6788	0.9780	8.7339
18c	1.9716	163.3276	0.7297	0.9811	8.5773
16a	2.0010	158.3042	*0.8295*	0.9209	7.6384
16b	2.0012	158.2721	0.8357	0.9240	7.6288
16c	2.0012	158.1718	0.8648	0.9237	7.6190
16d	2.0018	158.2111	0.8255	0.9248	7.6171
16e	2.0017	158.1106	0.8538	0.9250	7.6095
16f	2.0019	158.1078	0.8523	0.9289	7.6009
16-m	1.9545	164.2907	1.1116	0.9982	7.6769
20a	*1.9896*	162.3745	0.7095	*0.9661*	9.8805
20b	1.9908	162.1773	0.7104	0.9680	9.8609
20c	1.9900	161.8432	0.7619	0.9693	9.8431
20d	1.9909	162.1493	0.7295	0.9743	9.8420
20e	1.9893	161.6824	0.7874	0.9715	9.8257
20f	1.9929	161.6083	0.8503	0.9615	9.8152
20-m	1.9670	162.6020	0.9230	0.9859	9.9183
24a	1.9806	162.4897	*0.6226*	0.9646	12.0601
24b	1.9810	162.4365	0.6237	0.9675	12.0415
24c	1.9811	162.2174	0.6596	0.9706	12.0349
24d	1.9816	162.3450	0.6145	0.9713	12.0202
24e	1.9814	162.1247	0.6621	0.9724	12.0173
24f	1.9819	162.0243	0.6631	0.9734	11.9992
24-m	1.9737	161.6623	0.9189	0.9745	12.0784

[a] r_0 and θ_0 are bond length of O–H and bond angle of H–O–H in isolated water molecule at HF/6-311G(d,p) level.

energy than the distortion of bond angles when the water molecules are forming the clusters.

We also observe that the lowest-energy single-ring stacking structures with the stacking layers less than four (i.e, $(H_2O)_{8,10,12,15,18}$) are also the lowest-energy isomer of the corresponding clusters. However, the energies of four-layer single-ring stacking structures of $(H_2O)_{16,20,24}$ are not as good as of those of the two-layer multi-ring stacking isomers. As discussed above, the bond length of H-bond within the layers is shorter than that between the layers, suggesting that the strength of the H-bonds within the layers is stronger than that between the layers. We examine the ratio of the hydrogen bonds within the layers and between the layers, as well as the total number of hydrogen bonds in different isomers as shown in Table 2. From the strength of hydrogen bonding point of view, we can understand why the formation of 2-layer multi-ring stacking structures are energetically more favorable for $(H_2O)_{16,20,24}$. As shown in Table 2, all the multi-ring stacking structures have the ratio of the number of the hydrogen bonds within the layers and total number of H-bonds from 69.23 to 71.42%, much higher than the 57.14% in the corresponding 4-layer single-ring stacking structures. Although the total number of H-bonds in the multi-ring-stacking structures are less or equal to that of the corresponding 4-layer single-ring stacking structures, the larger number of stronger intra-layer hydrogen bonds can compensate the loss of some weaker inter-layer hydrogen bonds. We also note that for $(H_2O)_{12}$ the 3-layer 4-membered-ring stacking structure is better than the 2-layer hexamer stacking structure. That is because while both isomers have the same number (12) of stronger intra-layer H-bonds, the 3-layer isomer has two more inter-layer H-bonds than that of the 2-layer stacking isomer.

Conclusions

We have performed quantum chemistry calculations at the MP2/6-311++G(d,p)//HF/6-311G(d,p) level of theory to study the structures and stabilities of water clusters $(H_2O)_{8,10,12,15,16,18,20,24}$ with the ring stacking motifs. Our calculations show that in the single-ring stacking motif, the most stable isomers follow the alternative clockwise-anticlockwise stacking pattern, i.e., c-a, c-a-c, and c-a-c-a for two-, three-, and four-layer stacking isomers. We also show that four-layer single-ring stacking isomers are not energetically stable than those of two-layer multi-ring stacking isomers. The relative energetic stability is examined by analyzing the number and strength of H-bonds as well as bond lengths and bond angles distortions of the water molecules due to the formation of the clusters. We find that the strength of H-bonds within the layers is stronger than that between the layers. Therefore, the stability of the isomers is strongly correlated with the ratio of the number of H-bonds within the layers to total number of H-bonds in the cluster. We also find that the distortions in the water molecules will cost elastic energy which increase almost linearly with the bond length and bond angle distortions. Our study indicated the water tetramer, pentamer, and hexamer are good building blocks for assembling of larger water clusters. Although our present study focuses on the single-ring and multi-ring stacking motifs, most of the lowest-energy structures obtained from our calculations are also the lowest-energy structures, except for $(H_2O)_{16}$.

Computational Details

All calculations are performed using the GAUSSIAN-03 series of programs.[49] Geometry optimization of the water tetramer, pentamer, and hexamer are performed at the MP2/6-311++G(d,p) level of theory. The optimized structures of these three small clusters are shown in Figure 1. These optimized ring structures are then used to build the initial structures for the water clusters $(H_2O)_{8,10,12,15,16,18,20,24}$ based on different stacking sequences of single and multiple rings. The geometries of the water clusters, are then further optimized by the calculations carried out at the HF/6-311G(d,p) level of theory, followed by single point energy calculations at the MP2/6-311++G(d,p) level. The energy convergence criterion in all the calculations is set to be 10^{-8} Hartree.

Acknowledgements

The authors acknowledge the support by the National Natural Science Foundation of China under Grant Nos. 11574044 and the Fundamental Research Funds for the Central Universities. The calculations were also performed on TianHe-1(A) at National Supercomputer Center in Tianjin.

Conflict of interest

The authors declare no conflict of interest.

Keywords: ab initio calculations · hydrogen bonding · electronic structure · weak interactions · perturbation theory

[1] D. J. Wales, T. R. Walsh, *J. Chem. Phys.* **1997**, *106*, 7193–7207.
[2] D. J. Wales, T. R. Walsh, *J. Chem. Phys.* **1996**, *105*, 6957–6971.
[3] J. K. Gregory, D. C. Clary, *J. Chem. Phys.* **1996**, *105*, 6626.
[4] E. E. Dahlke, R. M. Olson, H. R. Leverentz, D. G. Truhlar, *J. Phys. Chem. A* **2008**, *112*, 3976–3984.
[5] B. Bandow, B. Hartke, *J. Phys. Chem. A* **2006**, *110*, 5809–5822.
[6] K. Kim, K. D. Jordan, T. S. Zwier, *J. Am. Chem. Soc.* **1994**, *116*, 11568–11569.
[7] J. Kim, K. S. Kim, *J. Chem. Phys.* **1998**, *109*, 5886–5895.
[8] C. J. Tsai, K. D. Jordan, *J. Phys. Chem.* **1993**, *97*, 5208.
[9] J. M. Pedulla, F. Vila, K. D. Jordan, *J. Chem. Phys.* **1996**, *105*, 1109.
[10] D. M. Bates, G. S. Tshumper, *J. Phys. Chem. A* **2009**, *113*, 3555–3559.
[11] K. Liu, J. D. Cruzan, R. J. Saykally, *Science* **1996**, *271*, 929–933.
[12] C. Pérez, M. T. Muckle, D. P. Zaleski, N. A. Seifert, B. Temelso, G. C. Shields, Z. Kisiel, B. H. Pate, *Science* **2012**, 336, 897–901.
[13] K. Nauta, R. E. Miller, *Science* **2000**, *287*, 293–295.
[14] M. Losada, S. Leutwyler, *J. Chem. Phys.* **2002**, *117*, 2003–2012.
[15] B. J. Mhin, J. Kim, S. Lee, J. Y. Lee, K. S. Kim, *J. Chem. Phys.* **1994**, *100*, 4484.
[16] J. K. Gregory, D. C. Clary, *J. Phys. Chem. A* **1997**, *101*, 6813.
[17] X. Meng, J. Guo, J. Peng, J. Chen, Z. Wang, J.-R. Shi, X.-Z. Li, E.-G. Wang, Y. Jiang, *Nature Phys.* **2015**, *11*, 235–239.
[18] C. Drechsel-Grau, D. Marx, *Nature Phys.* **2015**, *11*, 216–218.

[19] B. Wang, W. Jiang, X. Dai, Y. Gao, Z. Wang, R.-Q. Zhang, *Sci. Rep.* **2016**, *6*, 22099.
[20] B. Wang, W. Jiang, Y. Gao, B. K. Teo, Z. Wang, *Nano Res.* **2016**, *9*, 2782–2795.
[21] J. C. Howard, G. S. Tschumper, *WIREs Comput. Mol. Sci.* **2014**, *4*, 199–224.
[22] E. Miliordos, S. S. Xantheas, *J. Chem. Phys.* **2015**, *142*, 234303.
[23] C. J. Gruenloh, J. R. Carney, F. C. Hangeneister, C. A. Arrington, T. S. Zwier, S. Y. Fredericks, J. T. Wood III, K. D. Jordan, *J. Chem. Phys.* **1998**, *109*, 6601–6614.
[24] W. B. Blanton, S. W. Gorden-Wylie, G. R. Clark, K. D. Jordan, J. T. Wood, U. Geiser, T. J. Collins, *J. Am. Chem. Soc.* **1999**, *121*, 3551–3552.
[25] S. S. Xantheas, E. Aprá, *J. Chem. Phys.* **2004**, *120*, 823.
[26] C. J. Tsai, K. D. Jordan, *J. Chem. Phys.* **1991**, *95*, 3850.
[27] A. Khan, *J. Phys. Chem.* **1995**, *99*, 12450–12455.
[28] P. Bandyopadhyay, *Theor. Chem. Acc.* **2008**, *120*, 307–312.
[29] S. Maheshwary, N. Patel, N. Sathyamurthy, A. D. Kulkarni, S. R. Gadre, *J. Phys. Chem. A*, **2001**, *105*, 10525–10537.
[30] D. J. Wales, I. Ohmine, *J. Chem. Phys.* **1993**, *98*, 7257.
[31] D. J. Wales, I. Ohmine, *J. Chem. Phys.* **1993**, *98*, 7245.
[32] P. N. Day, R. Pachter, M. S. Gordon, G. N. Merrill, *J. Chem. Phys.* **2000**, *112*, 2063–2073.
[33] H. M. Lee, S. B. Suh, K. S. Kim, *J. Chem. Phys.* **2001**, *114*, 10749.
[34] J. Sadlej, *Chem. Phys. Lett.* **2001**, *333*, 485.
[35] A. Lenz, L. Ojamäe, *Chem. Phys. Lett.* **2006**, *418*, 361–367.
[36] G. S. Fanourgakis, E. Aprá, S. S. Xantheas, *J. Chem. Phys.* **2004**, *121*, 2655.
[37] S. McDonald, L. Ojamäe, S. J. Singer, *J. Phys. Chem. A* **1998**, *102*, 2824.
[38] L. S. Sremaniak, L. Perera, M. L. Berkowitz, *J. Chem. Phys.* **1996**, *105*, 3715.
[39] X. Liu, C.-W. Lu, C. Z. Wang, K. M. Ho, *Chem. Phys. Lett.* **2011**, *508*, 270–275.
[40] P. Qian, L. N. Lu, W. Song, Z. Z. Yang, *Theor. Chem. Acc.* **2009**, *123*, 487–500.
[41] T. James, D. J. Wales, J. Hernández-Rojas, *Chem. Phys. Lett.* **2005**, *415*, 302.
[42] H. Kabrede, R. Hentschke, *J. Phys. Chem. B* **2003**, *107*, 3914–3920.
[43] D. J. Wales, M. P. Hodges, *Chem. Phys. Lett.* **1998**, *286*, 65–72.
[44] G. S. Fanourgakis, S. S. Xantheas, *J. Phys. Chem. A* **2006**, *110*, 4100–4106.
[45] D. P. Tew, W. Klopper, *J. Chem. Phys.* **2005**, *123*, 07410.
[46] A. Halkier, W. Klopper, T. Helgaker, P. Jørgensen, P. R. Taylor, *J. Chem. Phys.* **1999**, *111*, 9157–9167.
[47] A. D. Boese, J. M. L. Martin, W. Klopper, *J. Phys. Chem. A* **2007**, *111*, 11122–11133.
[48] A. D. Kulkarni, V. Ganesh, S. R. Gadre, *J. Chem. Phys.* **2004**, *121*, 5043.
[49] M. J. Frisch, G. W. Trucks, H. B. Schlegel, G. E. Scuseria, M. A. Robb, J. R. Cheeseman, J. A. Jr. Montgomery, T. Vreven, K. N. Kudin, J. C. Burant, J. M. Millam, S. S. Iyengar, J. Tomasi, V. Barone, B. Mennucci, M. Cossi, G. Scalmani, N. Rega, G. A. Petersson, H. Nakatsuji, M. Hada, M. Ehara, K. Toyota, R. Fukuda, J. Hasegawa, M. Ishida, T. Nakajima, Y. Honda, O. Kitao, H. Nakai, M. Klene, X. Li, J. E. Knox, H. P. Hratchian, J. B. Cross, V. Bakken, C. Adamo, J. Jaramillo, R. Gomperts, R. E. Stratmann, O. Yazyev, A. J. Austin, R. Cammi, C. Pomelli, J. W. Ochterski, P. Y. Ayala, K. Morokuma, G. A. Voth, P. Salvador, J. J. Dannenberg, V. G. Zakrzewski, S. Dapprich, A. D. Daniels, M. C. Strain, O. Farkas, D. K. Malick, A. D. Rabuck, K. Raghavachari, J. B. Foresman, J. V. Ortiz, Q. Cui, A. G. Baboul, S. Clifford, J. Cioslowski, B. B. Stefanov, G. Liu, A. Liashenko, P. Piskorz, I. Komaromi, R. L. Martin, D. J. Fox, T. Keith, M. A. Al-Laham, C. Y. Peng, A. Nanayakkara, M. Challacombe, P. M. W. Gill, B. Johnson, W. Chen, M. W. Wong, C. Gonzalez, J. A. Pople, Gaussian 03, *Revision B. Gaussian, Inc., Pittsburgh, PA,* **2003**.

Manuscript received: December 7, 2018
Revised manuscript received: January 16, 2019